

# Galaxies at high redshifts – observing galaxies in the cradle

E. Thommes

Royal Observatory, Blackford Hill, Edinburgh, EH9 3HJ

**Abstract** Due to the invention of new powerful instruments in the recent past (e.g. 10m class telescopes) high redshift galaxies are no longer a curiosity. High redshift young star forming galaxies can be effectively discriminated from the much more abundant foreground galaxies by their special spectral properties: a prominent break at the Lyman limit (i.e. a complete absence of flux at wavelength below the Lyman limit), an intrinsically flat spectrum at wavelength long-ward of the Lyman limit and in the very early phase of evolution a strong Ly- $\alpha$  emission line with high equivalent width. In the last couple of years several hundred star forming galaxies with  $2.5 < z < 3.5$  could be identified using deep broad band images which identify the Lyman break (Steidel et al. 1996, 1998). Spectroscopic followup observations confirmed their high redshifts. I summarize the main properties of these Lyman break galaxies (LBGs). Furthermore, the very recent discoveries of very high- $z$  strong Ly- $\alpha$  emitting galaxies at  $z > 5$  and new large systematic surveys (the Calar Alto Deep Imaging Survey and the survey of Hu et al. 1998) for such objects, suggest that the cosmic star formation rate in strong Ly- $\alpha$  emitters does not decrease at redshifts  $z > 3.5$  as suggested for the Lyman break galaxy sample. I discuss the galaxies with the highest redshifts we know today and give an overview over the survey of Hu et al. and the Calar Alto Deep Imaging Survey.

## 1. Introduction

The most obvious boundary conditions for our understanding of how galaxies formed come from the observable properties of the galaxies itself.

Due to the invention of efficient instruments and large telescopes, e.g. large CCDs, NIR arrays, HST, Keck, etc. over the last couple of years we now begin to record the evolution of galaxies from their first star formation at very high redshift. In this context it is one of the great challenges of observational cosmology to detect the ancestors of normal present day galaxies (like our Milky Way) in the early universe which are in the stage of their first star formation. In the following, I call such objects *primeval galaxies* (PGs). The detection of a wide spread population of PGs would give us detailed information about several aspects of galaxy formation and would provide strong constraints for models of galaxy and structure formation in the universe.

Recent spectacular detections of young galaxies at  $z \geq 5$  (e.g. Dey et al. 1998, Weymann et al. 1998), the detection of a wide spread population of young galaxies at  $z = 3..4$  using color selection methods (Steidel et al. 1996) and new large survey projects for Ly- $\alpha$  emitting PGs at redshifts  $z > 5$  (the Calar Alto Deep Imaging Survey, Meisenheimer et al. 1998, and the survey of Hu et al. 1998), show that we are finally at the threshold where we are able to observe the earliest evolutionary phases of galaxies – galaxies in the cradle.

In this contribution I give an (biased) overview of the recent progress in observing young galaxies out to  $z \geq 5$ . The contribution is biased in the sense that I concentrate mainly on objects that we think could be the ancestors of normal present day galaxies.

The impatient reader may leap straight to Fig. 13, where I present an overview of a selection of individual objects and classes of objects with high redshift. After a discussion of the expected spectral features of young star forming galaxies at high- $z$  in section two, I discuss the main search techniques for high redshift galaxies in section three. In section four I present the search technique, the status and main properties of the Lyman break galaxies. In section five I discuss the search for strong Ly- $\alpha$  emitting galaxies at redshifts  $z > 5$  and give final remarks in section six.

## 2. Spectral features of young star forming galaxies at high $z$

Although the nature of the faintest galaxies detectable on deep direct CCD-exposures is still one of astronomy's grand questions (see the review of Ellis 1997), it is well known that

the majority of these objects are galaxies with redshifts below one. In order to distinguish between the bulk of these “foreground” galaxies and candidates for high-redshift galaxies ( $z \geq 2$ ), one has to find properties, which makes them different from the foreground objects. Therefore, let me first summarize the expected spectral features of high- $z$  young galaxies which can be used to identify them among the much more abundant foreground objects.

For redshifts  $z > 3$ , optical telescopes record the rest frame UV (1000 – 2000 Å). So one should look for interesting features expected for young star forming galaxies especially in their rest-frame UV. For every reasonable choice of the initial mass function of the newly forming stars the (rest-frame) UV spectral energy distribution of PGs should be dominated by the light of hot O and B stars. One could expect that the spectrum may have similar features as the UV spectra of giant HII regions in nearby galaxies. Thus, by studying the spectra of nearby star-forming galaxies (see e.g. Heckmann & Leitherer 1997) one should be able to learn something about the expected properties of PGs at high redshift. On the other hand, significant progress over the last years in modelling the evolution of stellar population in galaxies (see e.g. Charlot & Fall 1993) and the effects of the intervening intergalactic medium between us and the high- $z$  galaxies (Madau 1995), allowed to calculate detailed models of the expected spectral energy distributions. According to these models, the most important features of the observable spectral energy distribution of high redshift, young star forming galaxies are:

**(i) Strong Ly- $\alpha$  emission**

Population synthesis models of Charlot & Fall (1993) predict that a young, dust free, star-forming galaxy (without an AGN) should show strong Ly- $\alpha$  emission with (intrinsic) equivalent widths in the range of 50-250 Å. The flux in the Ly- $\alpha$  line is expected to be directly proportional to the actual SFR in the PG and 3 – 6 per cent of the bolometric luminosity are emitted in Ly- $\alpha$ . In the case of simple CASE B recombination and no dust, the Ly- $\alpha$  line is expected to be 8–11 times stronger than H $\alpha$ . On the other hand, because Ly- $\alpha$  photons are resonantly scattered, the probability that Ly- $\alpha$  photons are absorbed by dust is much higher than for continuum photons or photons of the Balmer lines. A Ly- $\alpha$  photon in an HII-region will be scattered  $10^6$  to  $10^7$  times before it leaves the HII-region (Osterbrock 1962). The optical path of a Ly- $\alpha$  photon to leave the HII-region is therefore  $\sqrt{N} \approx 10^3$  times longer than the direct path. Thus, even small amounts of dust in the plasma or in the surrounding HI-gas of the HII-region are able to eat most of the Ly- $\alpha$  photons away and could even lead to a negative Ly- $\alpha$  equivalent width (Chen & Neufeld 1994). But the effect of interstellar dust on Ly- $\alpha$  photons in connection with their resonant scattering is more complicated if the interstellar medium consists of multiple phases. For example, Neufeld (1991) showed that in a two phase interstellar medium Ly- $\alpha$  photons could be less absorbed by dust than continuum photons, resulting in even higher Ly- $\alpha$  equivalent

width than without dust. However, in the very first phase of star formation in galaxies, dust should not play a significant role. The presence of even small amounts of dust is a signature that one generation of stars has formed already. Therefore, strong Ly- $\alpha$  emission could be a selection criterion, to select the youngest objects, which are just in the stage of forming their first generation of stars, and which have not yet enriched their interstellar medium with dust. An additional factor which influences the detectability and especially the line profile of the Ly- $\alpha$  line of PGs is the velocity structure of neutral gas within the galaxies. As discussed above, relatively small column densities of neutral gas with even a very small dust content would destroy the Ly- $\alpha$  emission if this gas is static with respect to the ionized region where Ly- $\alpha$  photons originate from. The situation changes when most of the neutral gas is velocity-shifted with respect to the ionized regions (Kunth et al. 1998). For example, if the neutral gas surrounding the star-formation regions is outflowing from the ionized regions towards the observer, the resonant scattering would affect photons at shorter wavelengths than the Ly- $\alpha$  emission line, allowing the Ly- $\alpha$  photons to escape at least partially. Energetic out-flowing interstellar media are observed in the high redshift examples of Ly- $\alpha$  emitting star-forming galaxies (see section 4) as well in local star-burst galaxies observed with the Hubble Space Telescope (HST) and the Hopkins Ultraviolet Telescope (HUT) (Kunth et al. 1998; González Delgado et al. 1998).

**(ii) An intrinsically flat spectrum ( $F_\nu$ ) for  $\lambda > 912\text{nm}$  (=Lyman limit)**

The second special spectral feature expected for young star forming galaxies at high redshifts which is also predicted by population syntheses models (Charlot & Fall 1993) is a remarkable flat spectral energy distribution ( $F_\nu \approx \text{const}$ ) between the Lyman-limit and the Balmer-limit. This is due to UV-radiation from hot, short-lived ( $< 10^8\text{yr}$ ) massive stars. In the case of a constant star formation rate (SFR) an equilibrium between newly born and dying of these stars develops, so that their number stays constant (which is directly proportional to the SFR). Measuring the UV-flux of such a young star forming PG (which is redshifted into the optical or near-infrared for  $z > 2$ ) is therefore a direct measure of the instantaneous SFR within the system.

**(iii) A pronounced drop of the spectral energy distribution (SED) at the Lyman limit, e.g. a complete absence of flux at wavelength below the Lyman limit ( $\lambda < 912\text{nm}$ )**

This “Lyman break” has three causes:

- (a) There is an intrinsic drop in the spectra of hot O and B stars at the Ly-limit (Charlot & Fall 1993, Cassinelli et al. 1995). Furthermore, it is interesting that according to population syntheses models, the spectra of a burst stellar population with a declining

star formation rate of time scale  $10^7$  yr develops an extreme intrinsic Lyman break after about  $10^8$  years (Charlot & Fall 1993).

- (b) Absorption by the neutral interstellar medium in the galaxy itself (Leitherer et al. 1995a, 1995b, González Delgado et al. 1998)
- (c) Photoelectric absorption from neutral hydrogen in the Ly- $\alpha$  clouds and Ly-limit systems along the line of sight. Madau (1995) computed the HI opacity of a clumpy universe as a function of redshift, including scattering in resonant lines, such as Ly- $\alpha$ , Ly- $\beta$ , Ly- $\gamma$ , and higher order members, and Lyman-continuum absorption. At wavelengths short-ward of Ly- $\alpha$  in the emitter rest frame but long-ward of the Ly-limit, the source's continuum intensity is attenuated by the combined blanketing effect of many absorption lines of the Ly-forest (Ly- $\alpha$ , Ly- $\beta$ , Ly- $\gamma$ , Ly- $\delta$  ... line blanketing). Photons with wavelength shorter than the Ly-limit in the emitter rest frame suffer from photoelectric continuum absorption from neutral hydrogen in the systems along the line of sight.

### 3. Search techniques for high redshifted (primeval) galaxies

The expected spectral properties of young star forming galaxies at high redshifts discussed in the previous section lead to the following principle techniques to detect them in the optical/near infrared window  $0.32\mu\text{m} < \lambda < 2.4\mu\text{m}$ :

#### (A) Search for objects with prominent emission lines with narrow-band filters.

This requires the detection of emission line objects at a wavelength at which the redshifted lines (e.g. Ly- $\alpha$  or H $\alpha$ ) are expected. In order to keep the contrast with respect to the night sky and continuum dominated objects high, one uses narrow band imaging with a spectral resolution of a few hundred to several thousand  $\text{km s}^{-1}$ . Subsequent spectroscopic observations are necessary to establish whether the detected emission line is in fact the high redshift line one was searching for. The highest redshift PGs which could be detected from the ground by detecting their Ly- $\alpha$  emission line is given by redshifting this line to the upper boundary of the K-band window  $\lambda_{obs} \approx 2.3\mu\text{m}$  which corresponds to a redshift of  $z=18$ .

#### (B) Search for objects with unusual broad-band colours (using the Lyman break as a criterion).

This requires accurate broad-band photometry. The method was successfully introduced by Steidel et al. (1992,1993, 1996a,b) and will be discussed in section four.

- (C) **A hybrid method, combining accurate broad-band and medium-band photometry with a narrow band search for line emitting objects.** This allows one to get detailed information about the spectral energy distribution of the objects, which can be used to discriminate between foreground objects and good candidates for high redshift PGs. A survey based on this strategy is the Calar Alto Deep Imaging Survey (CADIS) (see section 5.3).

The next decision one has to take for a search for high redshift object is where to look for them. Several strategies are used:

(i) **“Guided” searches:**

The obvious targets for high- $z$  galaxy searches are fields in which high- $z$  objects are already detected. According to the paradigm of biased galaxy formation one would expect that the density of high- $z$  galaxies should be enhanced in this fields. Target fields for such “guided” searches have in the past been the fields of high- $z$  QSO’s, the fields of high- $z$  radio galaxies and searches at the redshifts of damped Ly- $\alpha$  systems. Ly- $\alpha$  emitting companions of quasars were indeed found (Djorgovski et al. 1985, Hu et al. 1991, Petitjean et al. 1996). Most of these are so close to the quasar, that their formation and excitation might be influenced by the quasar, so that they may not be representative of normal galaxies. But there have also been detections of high  $z$  Ly- $\alpha$  emitters in the fields of high- $z$  quasars which are too far away from the quasars to be influenced by the quasar itself (e.g. Hu and McMahon 1996). Damped Ly- $\alpha$  systems are thought to be signatures of disk galaxies in the line-of-sight towards the quasar and possible clusters of galaxies at that redshift. The search for high- $z$  emission line galaxies at the redshifts of damped Ly- $\alpha$  absorbers or strong metal absorbers of QSO’s were successful in several cases (e.g. Lowenthal et al. 1991, Macchetto et al. 1993, Giavalisco et al. 1994, Moller & Warren 1993, Djorgovski 1996, Francis et al. 1996, Mannucci et al. 1998).

(ii) **Search in “empty” fields:**

Fields suitable for the search of high redshift galaxies should not contain bright stars and should lie in a local minimum of the IRAS 100  $\mu\text{m}$  maps with e.g. absolute surface brightness less than 2 MJy/sr in order to avoid galactic extinction. Over the last few years several systematic survey projects for high redshift galaxies in “empty fields” have started and have already proved to be very efficient and successful. We will discuss some of these in section four and five.

- (iii) **Systematic search for high redshift galaxies in the surrounding of galaxy clusters.** The magnification due to gravitational lensing enhances the chance to

detect high redshift objects (see e.g. Franx et al. 1997)

**(iv) Serendipitous discoveries:**

As always in science, some important discoveries are serendipitous. For example, Dey et al. (1998) discovered a strong Ly- $\alpha$  emitting galaxy at  $z=5.34$  serendipitously during a successful search for  $z \approx 4$  galaxies using multi-colour techniques (see section 5.1).

## 4. Lyman break galaxies

### 4.1. Search technique and status

Based on the expected spectral property (iii) for high redshift star forming galaxies (as described in section 2 and 3) that they should show an obvious discontinuity in the far UV-spectrum at the limit of the Ly series near  $912 \text{ \AA}$  (the so called Lyman break), Steidel & Hamilton (1992, 1993) adopted a three filter system specifically tailored to detect this Lyman break in objects which are at  $z \approx 3$ . Fig. 1 illustrates how the 3 filters sample the far - UV continuum of a galaxy near  $z \approx 3$ . Two of the filters ( $U_n$  and  $G$ ) have passbands respectively below and above the Lyman-limit at  $z \approx 3$ , while the third filter,  $R$ , is further to the red. As Fig. 2 shows, in deep images of the sky taken through these three filters,  $z \approx 3$  galaxies are clearly distinguished from the bulk of lower redshift objects by their red ( $U_n - G$ ) and blues ( $G - R$ ) colours. Follow up spectroscopy with the Keck telescopes confirmed that this photometric selection technique is very efficient (Steidel et al. 1996a, 1996b). Approximately 80 % of the robust candidates turned out to be indeed high redshift galaxies, the remainder being mainly faint Galactic stars. Since then, large numbers of star forming galaxies at  $z \approx 3$  were discovered and confirmed using this technique (see e.g. Pettini et al. 1997 for a review). The Lyman break technique allows for the first time to assemble large samples of galaxies at previously inaccessible redshifts in order to study their properties and distribution. Steidel et al. (1998b) compiled a large sample of  $z \approx 3$  Lyman break galaxies (LBGs) selected in a consistent manner in 5 survey, fields each of size  $150\text{-}250 \text{ } \square'$ , which contain altogether  $\approx 1500$  LBG candidates (limiting magnitude  $R \leq 25 \text{ mag}$ ). They aim to confirm  $\approx 50\%$  of the candidates spectroscopically. Steidel et al. (1998b) claim to have 522 spectra of galaxies with  $z \geq 2.2$ , already (Mai 1998). The multi-colour method to select high- $z$  galaxies was also used in the Hubble Deep Field (HDF) and its flanking fields (see Dickinson 1998 for a review). The depth and the multi-colour nature of the HDF makes them ideal for this purpose.

Using different filter systems, the original Lyman break selection technique of Steidel

et al. can be extended to higher redshifts. Instead of looking for galaxies which exhibit the “break” in the  $U$ -band (“ $U$ -dropouts”,  $z \approx 3$ ) one can look for galaxies which show the Lyman break in the  $B$ -band (“ $B$ -dropouts”) implying  $z \approx 4$ . For example, Spinrad et al. (1998) used  $BVRI$  images of the field around the radio galaxy 6C0140+326 ( $z=4.41$ ; Rawlings et al. 1996) to select  $B$ -dropout candidates. They selected 13 potential  $B$ -dropout candidates from which they already could spectroscopically confirm 6 to be at redshifts between  $z=3.6$  and  $4.02$ . Steidel et al. (1998b) also used their  $G$  and  $R$  band filter images in connection with additional  $i$ -band images to select galaxies in the range  $3.9 \leq z \leq 4.5$  ( $G$ -dropouts). They also got confirming spectra of galaxies in this redshift range, although the sample is still much smaller than that for the  $U$ -dropouts. An investigation of the  $B$ -dropouts in the HDF was done by Madau et al. (1996). The remarkable result of their analysis is, that the space density of Lyman break galaxies seems to be significantly lower at  $z \approx 4$  than at  $z \approx 3$ . Madau et al. interpreted this as a declining cosmic star formation rate per comoving volume for  $z > 2.5 \dots 3.5$ . It will be important to check this result with further observations in larger fields from the ground, although the spectroscopic confirmation of galaxies at  $z \geq 3.5$  gets much harder because the spectral features useful for redshift identification move to wavelength  $\geq 6500 \text{ \AA}$ , where the sky is much brighter and the sky subtraction is more difficult. However, very recently Weymann et al. (1998) were able to spectroscopically confirm the redshift of a galaxy to be 5.60 which was selected as an “ $V$ -band dropout” in the HDF using the new NICMOS F110W ( $\sim J$ ) and F160W ( $\sim H$ ) data of the HDF together with the optical F606W ( $V$ ) and F814W ( $I$ ) HDF data. This shows that the multi-colour selection of high redshift objects using the Lyman break as a signature can be extended to very high redshifts, although the spectroscopic verification will get harder.

## 4.2. Properties of Lyman break galaxies

In the following I summarize the main observed properties of the LBGs at redshifts  $2.6 < z < 3.4$  observed by Steidel et al. (for details see Pettini et al. 1997, Steidel et al. 1998b, Dickinson 1998 and Adelberger et al. 1998).

### (A) Surface density and comoving space density:

The surface density of LBGs at  $R = 25\text{mag}$  which satisfy the colour criteria of Steidel et al. (see Fig. 1 and 2) is  $1.0/\text{arcmin}^2$ . This corresponds to a co-moving space density of  $2.2 \times 10^{-3} h_{70}^3 \text{Mpc}^{-3}$  for  $\Omega_m = 1$ , which corresponds roughly to the present day space density of galaxies with  $L > L^*$ . For  $\Omega_m = 0.2$  open or  $\Omega_m = 0.3$  flat (i.e.  $\Omega_\Lambda = 0.7$ ) the space density is roughly four times lower.

### (B) Clustering properties:

The redshift distribution of LBGs at  $z \approx 3$  shows significant “spikes” corresponding to structures on a scale of  $\approx 10$  Mpc (see Fig. 3). Such structures would be extremely rare if galaxy number density fluctuations were an unbiased tracer of matter fluctuations, and if one adopts a “cluster normalisation” for  $\sigma_8$  (e.g. from Eke, Cole and Frenk 1996). The existence of these “high peaks” requires a significant bias of the galaxy fluctuations as compared to the underlying mass fluctuations. From a count-in-cell measurement of 268 LBGs with spectroscopic redshifts in six  $9' \times 9'$  fields at  $z \approx 3$  Adelberger et al. (1998) deduced a bias on scales of  $\sim 10$  Mpc of  $b = \delta_{gal}/\delta_{mass} = 6 \pm 1$ ,  $1.9 \pm 0.4$  and  $4.0 \pm 0.7$  for  $\Omega_m = 1$ ,  $\Omega_m = 0.2$  open, and  $\Omega_m = 0.3$  flat respectively.

Both the number density (which reflect the power on scales of  $\sim 1$  Mpc) and the clustering properties (which reflect the power on  $\sim 10$  Mpc scales) together give constraints on the shape of the power spectrum of dark matter models of structure formation. According to these models, the large bias values are understandable, if individual LBGs would be associated with dark haloes with virial velocities of  $\approx 150$  km/s, similar to the dark haloes of massive galaxies at the present epoch.

### (C) Spectra of LBGs:

Fig. 4 shows some examples of spectra of LBGs. They show many similarities with those of nearby star-burst galaxies. A typical  $z \approx 3$  LBG with  $R \approx 24.5$ ,  $(G - R) \approx 0.5$  has a far UV luminosity of  $L_{1500} \approx 1.3 \times 10^{34} h_{70}^{-2}$  W/Å. This corresponds to a star formation rate (SFR) of  $\approx 8 h_{70}^{-2} M_{\odot}/\text{yr}$  (assuming a continuous star formation model with an age greater than  $10^8$  years and a Salpeter IMF from 0.1 to  $100 M_{\odot}$ , see e.g. Leitherer et al. 1995,  $H_0 = 70 h_{70} \text{ km s}^{-1} \text{ Mpc}^{-1}$ .) The spectra show strong low-ionization interstellar absorption lines e.g. SiII $\lambda$ 1260Å, OI $\lambda$ 1302Å, CII $\lambda$ 1335Å, FeII $\lambda$ 1608Å, AlII $\lambda$ 1670Å as well as high-ionization stellar absorption lines, often with P-Cygni line profiles characteristic of Wolf-Rayet and O star winds. Only 75% of the LBGs show Ly- $\alpha$  emission and always weaker than expected on the basis of the UV continuum luminosities. Some LBGs show Ly- $\alpha$  even in absorption. There are hints of a correlation between the strength of the metallic interstellar medium absorption and the strength of Ly- $\alpha$  absorption, and an anti-correlation with Ly- $\alpha$  emission (Spinrad et al. 1998). In the cases in which Ly- $\alpha$  is detected, the line is generally redshifted up to several hundred km/s relative to the interstellar absorption lines, and its profiles are clearly asymmetric, showing a P-Cygni type profile. This can be understood as originating from resonant scattering of the Ly- $\alpha$  photons in an out-flowing interstellar medium driven by mechanical energy generated in the star formation episode. As already mentioned above, similar effects are observed in nearby star forming galaxies.

### (D) Dust content of LBGs:

The UV spectral slope  $\alpha$  of LBGs ( $f_\nu \sim \lambda^\alpha$ ) are typically between 0 and +1.5 and therefore significantly greater than expected from spectral models which predict  $\alpha \approx -0.5 \dots 0$ . This can be explained if the spectra are reddened by dust extinction. Recently Pettini et al. (1998) presented the first five infrared spectra of LBGs in which they successfully detected Balmer and [OIII] emission lines. The detected H $\beta$  luminosities (uncorrected for dust extinction) implied star formation rates of  $20\text{--}270 h_{70}^{-2} M_\odot \text{yr}^{-1}$  which are significantly greater than those deduced from the UV luminosities at 1500 Å (see above). Although the sample is still very limited and uncertainties in the shape of the reddening curve and in the intrinsic UV continuum slope does not allow yet to determine the level of the dust extinction accurately, Pettini et al. estimated that an extinction of 1-2 magnitudes at 1500 Å may be typical for LBGs.

### (E) Speculations about the mass of LBGs

In four of the five galaxies for which Pettini et al. (1998) detected Balmer and [OIII] emission lines, they measured a velocity dispersion for the emission line gas of  $\sigma \approx 70 \text{ km/s}$ . With typical half-light radii of  $\approx 2 \text{ kpc}$  (deduced from HST NICMOS images as well as high resolution Keck images) Pettini et al. suggested virial masses for the LBGs in the range of  $M_{\text{vir}} \approx 1 - 5 \times 10^{10} M_\odot$  in contrast to dark halo masses of  $M_{\text{DM}} \geq 10^{11} M_\odot$  suggested from the number density and clustering properties (see above). But as Pettini et al. pointed out, it is possible that velocity dispersions (and therefore the masses deduced from them) have been significantly underestimated because the current limited sensitivity of the IR-spectra may only sample the inner cores of the galaxies, where the star formation rate is high.

## 4.3. What are the LBGs ?

For a detailed discussion of the interpretation of LBGs see the contribution of Mo in this proceedings. I want to mention here only two points:

(i) The number density and clustering properties of LBGs are consistent in all currently popular hierarchical models, if they are the central galaxies of the most massive dark matter halos present at  $z \sim 3$ .

(ii) The LBGs are not the long searched for primeval galaxies. They already formed at least one generation of stars which chemically enriched the systems and lead to dust formation, making Ly- $\alpha$  emission weak or undetectable. Earlier stages of evolution, before the formation of dust, may have much stronger Ly- $\alpha$  emission and fainter stellar continua than the LBGs at  $z \approx 2.5 \dots 3.5$  and may therefore be hard to pick out with the colour-break techniques, but relatively easy to find by searches for emission line objects. This is the

subject of the next section.

## 5. Search for Ly- $\alpha$ emitting high redshift galaxies

The systematic search for Ly- $\alpha$  emitting high redshift PGs has for a long time been a frustrating business without the success expected from early predictions (for a review see e.g. Pritchett 1994). But Thommes & Meisenheimer (1995, 1998, see also section 5.4 below) showed, that these searches were all based on far too optimistic predictions and that even the deepest surveys up to now had no realistic chance to find Ly- $\alpha$  emitting objects at high redshifts in large numbers.

Recently, a couple of strong Ly- $\alpha$  emitting galaxies at redshifts  $\geq 5$  have been discovered, and two new large survey projects which are much deeper and/or cover larger areas on the sky aiming to discover Ly- $\alpha$  emitters at redshifts  $z = 3...6$  have been started. One of these two surveys is the Calar Alto Deep Imaging Survey (CADIS) of the Max-Planck-Institut für Astronomie in Heidelberg, Germany (Meisenheimer et al. 1998, Thommes et al. 1997, 1998a). The second one is a survey of Hu & Cowie (1998) at the Institut for Astronomy in Hawaii. First results of these surveys, and the already mentioned recent discoveries of individual strong Ly- $\alpha$  emitters at redshifts of 4.92, 5.34 and 5.6, suggest that there might indeed exist an abundant population of strong Ly- $\alpha$  emitters at  $z \geq 5$  which might have a more “primeval signature” than the LBGs.

### 5.1. Examples of high redshift Ly- $\alpha$ emitting galaxies

As I mentioned in section 3, targeted searches for strong Ly- $\alpha$  emitters at the redshifts of quasars/radiogalaxies and the redshifts of absorption systems detected in quasar spectra, had been successful in several cases (e.g. Lowenthal et al. 1991, Macchetto et al. 1993, Giavalisco et al. 1994, Moller & Warren 1993, Djorgovski 1996, Francis et al. 1996, Pascarelle 1996, Hu & McMahon 1996). In 1997 Franx et al. reported the serendipitous discovery of two strong Ly- $\alpha$  emitting gravitationally lensed galaxies which they could spectroscopically confirm to be at a redshift of  $z=4.92$ . At that time these galaxies were the objects with the highest redshifts and for the first time the redshift record was not held by a quasar (the highest quasar redshift is still 4.897). One of the two galaxies is a prominent red arc visible in the HST images of the cluster CL1358+62. Franx et al. obtained Keck spectra of the arc, showing strong Ly- $\alpha$  emission at 7204 Å, a continuum drop blue-ward of the line and several absorption lines to the red. They reconstructed the image of the

high redshift galaxy using a gravitational lens model. The reconstructed galaxy image is asymmetric, containing a bright knot and a patch of extended emission 0.4 arcsec from the knot. This irregular structure is in contrast with the compact morphologies of the LBGs at  $z \approx 3$  (Giavalisco et al. 1996). The galaxy has a luminosity  $I_{AB} \approx 24$  mag, which could be produced by a star formation rate of  $18 \text{ h}_7^{-2} 0 \text{ M}_\odot \text{ yr}^{-1}$  ( $q_0 = 0.5$ ). The spectral lines show velocity variations on the order of 300 km/s along the arc. The Ly- $\alpha$  emission line is asymmetric with a red tail and the Si V line is blue shifted with respect to Ly- $\alpha$ . These characteristic features already well known from the LBGs (see above) again indicate that radial outflows dominate the kinematics of the absorption line gas. The second galaxy Franx et al. confirmed to be at  $z = 4.92$  is a companion galaxy with a radial velocity of only  $450 \text{ km s}^{-1}$  different than that of the arc. Although these two galaxies with  $z = 4.92$  were the first objects which beat the quasars in redshift, they were soon beaten by an other serendipitous discovery of a strong Ly- $\alpha$  emitter at  $z=5.34$  by Dey et al. (1998). This galaxy was the first object spectroscopically confirmed to be at  $z>5$  and was discovered during a successful search for  $z \sim 4$  LBGs (*B*-dropouts) (see Fig. 5). Fig. 6 shows the spectrum of this  $z=5.34$  Ly- $\alpha$  emitter, which is exposed 36200 s with the Low Resolution Imaging Spectrometer (LRIS; Oke et al., 1995) on the Keck telescope. The strong emission line is asymmetric, as expected for Ly- $\alpha$  lines in high redshifted young star forming galaxies, and the spectrum shows a weak continuum emission ( $= 27\text{AB mag}$  for  $7735 \text{ \AA} < \lambda_{obs} < 9000 \text{ \AA}$ ) red-ward of the line and no flux detection (upper limit  $= 29.5\text{AB mag } 1\sigma$ ) blue-ward of the line ( $6200 \text{ \AA} < \lambda_{obs} < 7700 \text{ \AA}$ ). Dey et al. measured a “flux-deficit” parameter <sup>1</sup> for this discontinuity at the emission line of  $D_A > 0.70$  ( $3\sigma$  lower limit) which is consistent with the theoretical estimate of  $D_A(z=5.34)=0.79$  of Madau (1995) for a galaxy at  $z=5.34$ . Furthermore, because there are no other lines detected in the spectrum, there are just two possible interpretations for the emission line: [OII] $\lambda\lambda 3726, 3729$  ( $z=1.07$ ) or Ly- $\alpha$  ( $z=5.34$ ). In case of [OII] at  $z=1.07$ , the rest frame equivalent width would be  $\approx 300 \text{ \AA}$ , which is in excess of what is produced by even the most luminous star-forming galaxies (typical less than  $70 \text{ \AA}$ , Liu & Kennicutt, 1995). In addition, Dey et al. tried to fit the observed line profile with an [OII] $\lambda\lambda 3726, 3729$  doublet which resulted in a  $3726/3729$  ratio of  $>2$  which is unphysical (the highest allowed is 1.5). Thus, the only interpretation for the emission line is indeed Ly- $\alpha$  and therefore the redshift of  $z=5.34$  is secure. The relatively narrow Ly- $\alpha$  line (deconvolved FWHM  $\approx 280 \text{ km s}^{-1}$ ), the rest frame Ly- $\alpha$  equivalent width of  $\approx 95 \pm 15 \text{ \AA}$ , and the lack of strong emission of NV  $\lambda\lambda 1239, 1243$  and SiIV  $\lambda\lambda 1394, 1403$ , suggest that this is a star-forming galaxy and not an AGN. The star-formation rates deduced from the UV

---

<sup>1</sup>which is defined as  $D_A = < 1 - \frac{F_\nu(\lambda 1050-1170)_{obs}}{F_\nu(\lambda 1050-1170)_{pred}} > . D_A$  describes the discontinuity at the Ly- $\alpha$  line due to absorption in foreground intervening systems. The predicted flux is the flux level one would expect without this absorption.

continuum emission and the Ly- $\alpha$  emission coincides and gives a  $\text{SFR} \approx 3M_{\odot}/\text{yr } h_{70}^{-2}$  (for  $q_0 = 0.5$ ). Although the deduced SFR is comparable to the SFR observed in the LBGs, the fact that the SFR implied by  $L_{1500}$  is very similar to that derived from  $L_{Ly\alpha}$  shows, that this object is not significantly attenuated by dust, in contrast to the LBGs (see above). Furthermore, the galaxy at  $z=5.34$  discovered by Dey et al. is spatially resolved in the ground-based I-band images. Although the observed morphology may be dictated by the Ly- $\alpha$  emission line (which is contained in the I-band filter), this is again differing from the LBGs at redshifts 2.5–3.5, which are compact systems with half-light radii  $\sim 0.2\text{--}0.3$  arcsec (Giavalisco et al. 1996). These differences could be understood, if the galaxy at  $z=5.34$  is in an earlier stage of evolution, than the LBGs.

At the time of the writing of this contribution (October 1998) the redshift record has already been pushed beyond  $z=5.34$ . As I mentioned above, Weymann et al. (1998) selected a galaxy on the new HST NICMOS J and H images of the HDF which could be spectroscopically confirmed to be a strong Ly- $\alpha$  emitter at  $z=5.60$ . Furthermore, Hu et al. (1998) claim to have found a strong Ly- $\alpha$  emitter at a redshift of  $z=5.64$  in their survey (see below).

## 5.2. Blank-field survey for high- $z$ Ly- $\alpha$ emitters of Hu et al. (1998)

Using the 10m Keck II telescope, Hu, Cowie & McMahon (1998) recently started a narrowband and spectroscopic search for strong Ly- $\alpha$  emitting star forming galaxies in the redshift range 3–6. They reach extremely faint flux levels of  $\approx 1.5 \times 10^{-20} \text{ W/m}^2$  ( $5\sigma$ ). Their main selection criterion to discriminate high redshift Ly- $\alpha$  candidates from foreground emission line objects is an extremely high equivalent width of the emission line ( $W_{\lambda} > 100 \text{ \AA}$ ) together with additional broad-band colour criteria. As a first step, they performed deep narrow band images with a 5390/77  $\text{\AA}$  filter together with deep broad band  $B, V$  and  $I$  data in the HDF and the Hawaii Deep Field SSA22 with the LRIS instrument at the Keck II 10m telescope (see Cowie et al. 1998). Using the redshift information available for many objects in the HDF and SSA22, they demonstrated how certain criteria on the  $(V - I)$  and  $(B - V)$  colour can help to discriminate between the three main classes of strong emission lines [OII], [OIII] and Ly- $\alpha$ , that can produce significant equivalent widths in the narrow band. Using these colour criteria together with the equivalent width criterion ( $W_{\lambda} > 100 \text{ \AA}$  in the 5390/77  $\text{\AA}$  filter), they selected a sample of 12 objects in the SSA22 and HDF fields. Among these 12 objects is the Ly- $\alpha$  emitting object, whose redshift was already confirmed to be at  $z = 3.4$  by Lowenthal et al. (1997). Multi-object spectroscopy of the objects with LRIS on Keck II confirmed the strong emission lines to be Ly- $\alpha$ . Some of these Ly- $\alpha$

emitters show continuum colours similar to those of the colour-selected LBGs (which is not surprising). However, the most interesting result is that the sample also contains objects with very faint continua, that would have fallen below the magnitude threshold of current LBG surveys. Two of the objects could not even be detected in the broad band images at all ( $1\sigma$ ,  $B=27.8$ ,  $V=27.5$ , and  $I=25.8$ ) with  $W_\lambda > 400 \text{ \AA}$ . Although the covered field of  $46 \text{ arcmin}^2$  and redshift range of  $3.405\text{--}3.470$  is very small, Cowie and Hu (1998) deduce from their detections that the number density of strong Ly- $\alpha$  emitters at  $z \approx 3.5$  with flux  $> 2 \times 10^{-20} \text{ W/m}^2$  could be as high as  $13000/\text{unit } z/\text{ }^\circ$  of which an essential fraction has too faint continua to be selected by current LBG surveys.

Hu, Cowie & McMahon extended their search for Ly- $\alpha$  emitting galaxies at high  $z$  by observing the SSA22 field through a narrow-band interference filter centered at  $6741 \text{ \AA}$  with a bandpass of  $78 \text{ \AA}$ , corresponding to a Ly- $\alpha$  redshift of  $z \approx 4.52$ . They selected 3 emission line objects with observed equivalent width of  $W_\lambda > 100 \text{ \AA}$ . To discriminate between the most likely interpretations of the emission line ([OII] $\lambda 3727$  at  $z = 0.8$ , [OIII] $\lambda\lambda 4959, 5007$  or H $\beta$   $\lambda 4861$  at  $z=0.37$ , H $\alpha$   $\lambda 6563$  at  $z = 0.03$  or Ly- $\alpha$  at  $z = 4.52$ ), Hu et al. did spectroscopic follow up observations of all the candidates. The lowest flux object with the weakest equivalent width ( $W_\lambda \approx 120 \text{ \AA}$ ) could be identified as an [OII] emitter at  $z=0.814$  and the other two are indeed most likely Ly- $\alpha$  emitters at  $z = 4.52$ .

In addition to these narrow band searches, Hu et al. examined older spectroscopic data taken for other purposes, in order to search for serendipitous high redshift Ly- $\alpha$  emitters. The data (slit spectra with LIRS on the 10m Keck telescope) covered a blank sky area of  $\approx 200 \text{ }^\circ$ , covered a spectral range corresponding to Ly- $\alpha$  redshifts of  $z=3.04\text{--}5.64$ , and reached a detection limit of  $1\sigma \sim 10^{-21} \text{ W/m}^2 \text{ s}^{-1}$ . In this data set they found 4 high equivalent width objects which show hints of a break at the line. If the lines they detect are indeed Ly- $\alpha$ , the redshifts would be  $z = 5.64, 4.19, 4.02, 3.05$ . However, especially the spectrum of the probably  $z = 5.64$  object is not good enough to be completely sure that the detected line is Ly- $\alpha$ . The spectra do not have the necessary S/N to see e.g. the expected asymmetry of a high  $z$  Ly- $\alpha$  line, to see the doublet structure in case of [OII], or to measure the flux decrement  $D_A$ , like it was possible in the spectrum of the  $z=5.34$  Ly- $\alpha$  emitter discovered by Dey et al. (1998). Additional spectroscopic data is necessary.

However, this first results of the Hu et al. survey show that Ly- $\alpha$  emitting galaxies at high redshifts are quite common objects with a significant contribution to the cosmic star formation rate. Although the covered area is still much too small to draw conclusions there are already hints that the cosmic star formation rate in the strong Ly- $\alpha$  emitters is probably constant or even increasing with redshift from  $z = 3 - 6$ , in contrast to colour-based LBG samples where the rate seems to be declining at higher redshifts (Madau et al. 1996, 1998).

However, this has to be proven by additional data. We started a large emission-line survey for high- $z$  Ly- $\alpha$  emitting primeval galaxies ( $z=4.7, 5.7, 6.5$ ) at the Max-Planck Institut für Astronomie in Heidelberg, called the Calar Alto Deep Imaging Survey (CADIS), which covers a much larger area on the sky ( $\approx 0.3^\circ$ ) reaching flux limits of  $3 \times 10^{-20} \text{ Wm}^{-2}$ . With its large area coverage CADIS complements the deeper Hawaii survey and both together will give interesting constraints for the number density of Ly- $\alpha$  emitting primeval galaxies at  $z > 5$ .

### 5.3. The Calar Alto Deep Imaging Survey

#### 5.3.1. The CADIS concept

The Calar Alto Deep Imaging Survey (CADIS) is the current extragalactic key-project of the Max-Planck-Institut für Astronomie (see Meisenheimer et al. 1995, 1998, Thommes et al. 1997)<sup>2</sup>. CADIS is a very deep emission line survey using an imaging Fabry-Pérot, combined with deep broad- and medium-band photometry. This survey project is specifically designed to detect Ly- $\alpha$  emitting primeval galaxies (PGs) at redshifts  $z \geq 5$ , but it will in addition produce a large data base for investigations of the faint end of the luminosity function and the three dimensional correlation function of faint emission line galaxies at intermediate redshifts ( $0.2 < z < 1.2$ ). Its multifilter technique also allows the classification and redshift determination of several hundred early type galaxies at  $0.5 < z < 1.2$  (which will complete the luminosity function at the bright end), to detect faint QSOs beyond  $z = 3$  and even beyond  $z = 5$ , to select extremely red objects (EROs) with  $R - K' \geq 6$ , and of faint M stars and faint brown dwarfs.

The central point of the strategy is the search for faint emission line objects ( $S_{lim}(5\sigma) \approx 3 \times 10^{-20} \text{ W/m}^2$ ) with an imaging Fabry-Pérot in the wavelength intervals (A) [694,706nm], (B) [814,826nm] and (C) [910,926nm]. These wavelength intervals are located in prominent windows of the night sky emission, corresponding to Ly- $\alpha$  redshifts of  $z=4.75, 5.75$  and  $6.55$ . The very deep flux limit for line detection allows one to detect star formation rates (SFRs) of 10 to 50  $M_\odot/\text{yr}$  in PGs at  $z \geq 5$ . A completely new feature of the CADIS strategy are very deep images in a set of narrow band filters ( $R = \lambda/\Delta\lambda \approx 50$ , typical exposure times: 10 h at a 2.2 m telescope), which are selected in such a way, that for every prominent emission line of a foreground object falling into the Fabry-Pérot scan (e.g.  $H\alpha$ )

---

<sup>2</sup>Participating scientists: S. Beckwith, F.H. Chaffee, R. Fockenbrock, J. Fried, H. Hippelein, U. Hopp, J. Huang, Ch. Leinert, K. Meisenheimer, S. Phleps, H.-J. Röser, I. Thiering, E. Thommes, D. Thompson, B. von Kuhlmann, C. Wolf

a second or third line (e.g. [OII]372.7nm or [OIII]500.7nm ) should show up in them (fig. 7). We call these narrow band filters veto-filters since a signal in one of them excludes that the line detected in the Fabry-Pérot is Ly- $\alpha$ . Combining the veto-filter information with the accurate spectroscopy through the Fabry-Pérot, we expect to determine the redshift of the majority of emission line galaxies ( $0.25 < z < 1.0$ ) to an accuracy of 100 ... 200 km/s (depending on the S/N ratio). Since the detection of emission line objects requires several “off-line” continuum exposures anyway, we decided to add in a complete set of broad band and medium band images, which are optimized both for the continuum determination and the identification of one of the most severe contaminations - faint M-stars in our Galaxy. The optical multi-color survey is supplemented by a  $K'$  ( $5\sigma$  limit 21.0 mag) survey with the new OMEGA camera at the prime focus of the Calar Alto 3.5 m-telescope ( $6.6 \times 6.6 \square'$  field). This gives us a global view of the spectral energy distribution (SED) of every object in the field. The narrow band and medium band images will allow us to discriminate very effectively between foreground emission line objects and good candidates for Ly- $\alpha$  emitting PGs at high redshifts (Fig. 7). CADIS will survey 10 fields (each  $120 \square'$ ) distributed over the northern sky ( $\delta \geq -5^\circ$ ), which were selected for their absence of bright stars ( $R \leq 16.0$ ) and an extra-ordinary low flux in the IRAS  $100\mu\text{m}$  maps ( $\leq 2 \text{ MJy/sr}$ ). Thus, the total survey area will be at least  $0.3 \square^\circ$ . CADIS will use the 2.2m- and the 3.5m-telescopes at Calar Alto (Spain).

### 5.3.2. *Current status of the survey*

About 1/3 of the survey data have been collected in the two years since regular survey observations commenced at the Calar Alto 2.2m and 3.5m telescopes. Delays in the delivery of the Fabry-Pérot-etalon for the 3.5m focal reducer, however, have caused a large backlog in the central part of CADIS - the deep emission line survey. Up to now, we have only been able to collect reasonably complete data sets for two northern fields at RA=09h and 16h.

### 5.3.3. *Primeval galaxies at $z > 5$ - problems and first candidates*

Due to the delay in the delivery of the Fabry-Pérot etalon for the 3.5m focal reducer the emission line survey is far behind our original schedule. In addition, we recently discovered that the original flat field corrections of the Fabry-Pérot images were severely flawed by internal reflections between the etalon and the focal reducer optics, which causes a central “hump” in the images. Treating this central “hump” as a (multiplicative) flat field property thus artificially enhanced the measured flux in the Fabry-Pérot bands in the

outer regions by  $> 20\%$ . We subsequently developed a method by which an additional calibration through a multi-hole mask inserted at the telescope focus is used to calibrate the transmission properties of the entire optical system focal reducer-etalon-prefilter. The central hump (which is also present on night sky science exposures) is then treated as sky concentration and subtracted from the science exposures. Previously, we presented a list of seven Ly- $\alpha$  candidates, drawn from an early analysis of first CADIS observations in the 9h field (Thommes et al. 1998a). However, a reanalysis of the data with the improved flat field correction, together with new Fabry-Pérot and veto-filter observations as well as spectroscopic follow-up observations of some of the candidates with the Keck 10m telescope, showed that none of these candidates is a genuine Ly- $\alpha$  galaxy at redshift  $z = 5.7$  (for details see Thommes et al. 1998b). One of the candidates seems to be an emission line object which is located at  $z \approx 0.25$ . The remaining 6 objects are most likely instrumental artifacts which have been caused by the imperfect flat field correction of the Fabry-Pérot data in the first analysis. There seems to be no emission line objects detected in the 9h field, which cannot be identified as a foreground galaxy by means of the veto filter observations or a significant signal on the deep blue band exposures. That the CADIS Fabry-Pérot and narrow band data are indeed able to identify the emission lines and to determine the redshift of the faint foreground emission line objects, is demonstrated in Fig. 8.

Applying the improved data reduction procedure to the - much more complete - Fabry-Pérot and veto filter data of the 16h field yields two Ly- $\alpha$  candidates, one of which appears uncertain due to its proximity to a rather bright stellar object ( $R=19.6$ ). In summary, we are currently left with  $1 \pm 1$  Ly- $\alpha$  candidate at  $z = 5.7$  in a search volume corresponding to one complete CADIS field (7 wavelength settings in 16h field and 3 settings in the 9h field in wavelength region B [814,826nm]).

#### 5.3.4. *Surface density of Ly- $\alpha$ emitting galaxies at high redshifts*

Assuming that there are in any case less than 3 Ly- $\alpha$  emitting PGs at  $z=5.7$  in our 9H and 16H field data, we get the limit marked in Fig. 9. For comparison, the small points with the error bars correspond to the candidates reported by Cowie and Hu (1998) for Ly- $\alpha$  emitters at  $z=3.4$ . If the detection of the very high surface density of Ly- $\alpha$  emitting galaxies by Cowie and Hu (1998) and Hu et al. (1998) at  $z=3.4$  and 4.5 as shown in Fig. 9 will be confirmed, the limits posed by our non-detection of PGs in the small subset of CADIS data may give challenging constraints for models of the surface density of Ly- $\alpha$  emitting galaxies at high redshift. The curves in Fig. 9 show the results of such model calculations. We trimmed the free parameters (see Thommes & Meisenheimer, 1998c) to get results which

are consistent with our limits and the observations of Cowie and Hu (1998). The models predict that the number density of Ly- $\alpha$  galaxies should not change very much in the redshift interval  $z_0 = 3.5$  to 4.5 at low detection limits of  $S_{lim} \leq 2 \times 10^{-20}$  W/m<sup>2</sup>. This is consistent with the claims of Hu et al. (1998), that the surface density of Ly- $\alpha$  emitters at these detection limits is as high as  $\approx 1500/\square^\circ/\Delta z = 0.1$  at  $z_0 = 3.5$  **and** 4.5. At detection limits above  $S_{lim} \geq 2 \times 10^{-20}$  W/m<sup>2</sup> the expected number density decreases rapidly with increasing  $z_0$ , consistent with the null detection in the recent subset of CADIS data. At redshifts  $\geq 6.0$ , the models predict surface densities which are much lower than at  $z_0 = 3.5$  for all detection limits  $S_{lim} \geq 10^{-20}$  W/m<sup>2</sup>. However, much more data in more fields is needed to draw definite conclusions about the mean surface density of Ly- $\alpha$  emitting galaxies at high redshifts. Especially, if Ly- $\alpha$  galaxies at  $z \geq 3.5$  have similar clustering properties as the colour selected Lyman break galaxies, the number density of Ly- $\alpha$  emitters in the CADIS data and the data of Cowie and Hu may be substantially influenced by clustering. Steidel et al. (1998) found high spikes with relative overdensities of up to 2.6 in the distribution of Lyman break galaxies in volumes of comoving size  $\approx 10^3 h_{100}^{-3}$  Mpc<sup>3</sup> (see section 4.2). The 9H CADIS data cover a comoving volume of  $27.1 \times 27.1 \times 12.7 h_{70}^{-3}$  Mpc<sup>3</sup> in the case of  $q_0 = 0.1$  and  $14.6 \times 14.6 \times 7.1 h_{70}^{-3}$  Mpc<sup>3</sup> in the case of  $q_0 = 0.5$ . Thus, clustering may substantially influence the number density of high- $z$  Ly- $\alpha$  emitters observed in single CADIS fields. To average these effects out, one has to observe many fields and/or larger redshift intervals. CADIS will search for Ly- $\alpha$  emitting galaxies in 9 fields each of  $\approx 120 \square'$  at redshifts 4.75, 5.75 and 6.55 with coverage of  $\Delta z = 0.1$  each. This should give a firm basis to investigate the average number density of Ly- $\alpha$  emitting galaxies at high redshifts and may produce strong constraints for models of galaxy formation.

### 5.3.5. Other interesting first CADIS results: High- $z$ QSOs and EROs

CADIS identifies QSOs either by their peculiar colours or their variability over a period of several years. The complete optical filter set of the survey is displayed in Fig. 10.

CADIS employs a completely new approach for classification and redshift estimation from multi-colour data. Essentially it is based on a comparison between the *observed* colours of any objects detected in the survey with the “reference colours” of tens of thousands of template spectra of stars, galaxies and QSOs of different type and redshift (for details see Wolf, C. et al. 1998). Applying this method to the data of three CADIS fields of 225  $\square'$  total area, we selected 26 objects with AGN-like colours. Spectroscopic followup observations confirmed 22 of the 26 candidates as broad-line AGNs, whereas three turned out to be stars and one is a narrow emission-line galaxy. Five of the 22 AGNs have luminosities below

$M_B = -23$  mag ranking them as Seyfert-1 galaxies, while the other 17 are genuine quasars. Among these, 16 are brighter than  $R = 22$  mag and half of them are located at  $z > 2.2$ . Our results for the surface density of  $z < 2.2$ -quasars are consistent with published values, but at  $z > 2.2$  the CADIS number exceeds published values (see Fig. 11). This is a very interesting result, which challenges the general belief that the quasar number density drops off at higher redshift, as suggested by previous surveys (see review of Hartwick & Schade, 1990). Obviously, CADIS finds high-redshift quasars with unprecedented completeness. An explanation for the fact that other surveys miss many of the quasars with redshifts higher than 2.2, which CADIS is able to find, is that many of these quasars found in CADIS display rather star-like colours in broadband filters, and would not have been picked out in classical multi-colour surveys.

Another interesting result of CADIS is the detection of many extremely red objects (EROs,) defined by their  $R - K' \geq 6$ . To date we have observed 4 CADIS fields, each covering  $\approx 160$  arcmin<sup>2</sup> to a  $5\sigma$  limit of  $K'=20.5$  mag. Combining these data with the CADIS  $R$ -band data ( $2\sigma$ -limit = 26.0 mag), we have selected complete, unbiased, magnitude-limited samples of EROs (see Fig. 12). We find a surface density of EROs with  $K' \leq 20.0$  mag of 0.33 arcmin<sup>2</sup> and for EROs with  $K' \leq 19.0$  mag of 0.039 arcmin<sup>2</sup> (see Thompson et al. 1998). Two alternative interpretations have emerged to explain the extremely red spectral energy distributions (SEDs) of these galaxies. Initially, an old stellar population, such as found in present-day elliptical galaxies, provided a good fit to the SEDs. A strong, redshifted 4000 Å break falling between the  $R$  and  $K$  filter bandpasses and the lack of any appreciable restframe UV light from a young population of stars are responsible for the extremely red colors. The alternative interpretation is that these galaxies are star-bursts or active galactic nuclei (AGN), perhaps triggered by a merging event. In this scenario, the presence of significant quantities of interstellar dust hides the star-forming regions or AGN, considerably reddening the observed SEDs. In both cases, the galaxies are most likely to lie at redshifts  $0.8 < z < 2.0$ . Because EROs appear to be very common objects, both interpretations of the red colors of EROs have significant implications for our understanding of galaxy formation and evolution. If the ERO population is dominated by old ellipticals, then massive galaxy formation was well underway at  $z > 3$ . Dust-dominated EROs, however, imply that much of the massive galaxy formation could actually occur at late times, supporting hierarchical galaxy formation models. To investigate the ERO population further and to decide which fraction of the EROs are dusty star forming galaxies and which fraction are maybe old ellipticals, we already begun some additional follow-up work. This includes deeper, higher-resolution images and photometry and additional observations at various wavelengths, e.g. with SCUBA in the submillimeter.

## 6. Final remarks

In Fig. 13 I present an overview of individual objects and classes of objects at high redshift we know today (the list of objects is certainly not complete). Many of the displayed objects were “touched” in this review, others were not, e.g. I did not discuss high- $z$  radio galaxies and only briefly mentioned the QSOs in connection with the interesting CADIS result.

Fig. 13 also includes the “Madau-plot” (which is cited so often these days and which I reproduced here from Pettini et al. 1997) showing estimates of the star formation history in the universe. The filled points are the original points which Madau (1997) deduced from combining the results of the complete redshift surveys reaching  $z \approx 1$  (e.g. Lilly et al. 1995, review of Ellis 1997) with the star formation rates and number densities of the LBGs. However, the original curve first presented by Madau has been the subject of intensive discussion. There are several observational facts which suggest that the points have to be corrected upwards and that the cosmic star formation rate may not drop as fast at  $z > 3$ . Note that, as discussed in section 4.2, the LBGs are already dusty. Taking dust absorption into account gives the higher (open) points in Fig. 12 (see Pettini et al. 1997). Furthermore, the detection of a population of strong Ly- $\alpha$  emitters out to redshifts of 6 (see chapter 5), which are partly missed by the Lyman break technique, may suggest that the cosmic star formation rates have to be corrected further upwards at these redshifts (as I indicated by the arrow). And last but not least, there might be a population of star forming galaxies at high- $z$ , which are completely obscured by dust and therefore not detectable in the optical/near infrared regime. Such objects could be detected in the far-infrared and sub-millimetre due to their dust emission. New instruments like SCUBA on the JCMT allow for the first time deep submm-surveys of blank sky regions. First results of such SCUBA surveys (see Hughes et al. 1998, Barger et al. 1998) indeed found significant number densities of submillimetre sources, which are most likely starbursting galaxies in the redshift range  $2 < z < 4$ .

The study of high redshift galaxies is a rapidly improving field of research and the future promises to be even more exiting. With new instruments like the Next Generation Space Telescope it may even be possible to observe supernovae explosions from massive star bursts out to  $z = 10$ . Theoretical models of galaxy and structure formation will be more and more constrained by direct observations of the evolution of galaxies starting from their first emission of star light in the cradle to the grown up systems they are today.

I am grateful to G. Boerner and H. Mo for the invitation to the workshop, to E. van Kampen and J. Peacock for comments on a draft of this article and to the Deutsche

Forschungsgemeinschaft for the research fellowship supporting my stay at the Royal Observatory in Edinburgh.

## REFERENCES

- Adelberger, K.L. et al., 1998, ApJ, 505, 18
- Barger et al., 1998, Nature, 394, 248
- Boyle B.J. et al. 1991, eds. Barrow J. D., Mestel L., Thomas P. A., in *Texas/ESO-CERN Symposium on Relativistic Astrophysics Cosmology, and Fundamental Physics* NYAS Vol. 647, p. 14
- Cassinelli et al., 1995, ApJ, 438, 932
- Charlot, S. & Fall, S., 1993, ApJ, 415, 580
- Chen, W. & Neufeld, D., 1994, ApJ, 432, 567
- Cowie, L.L. & Hu, E.M., 1998, AJ, 115, 1319
- Dey, A. et al., 1998, ApJ, 498, L93
- Dickinson, M., 1998, astro-ph/9802064
- Djorgovski et al., 1996, Nature, 382, 234
- Djorgovski et al., 1995, ApJ 299, L1
- Eke, V.R., Cole, S., & Frenk, C.S., 1996, MNRAS, 282, 263
- Ellis, R.S., 1997, AAR&A, 35, 389
- Francis, P.J. et al., 1996, ApJ, 457, 490
- Franx, M., et al., 1997, ApJ, 486, L75
- Giavalisco, M., et al., 1996, ApJ, 470, 189
- Giavalisco, M., et al., 1994, A&A 288, 103
- González Delgado, R.M., et al., ApJ, 1998, 495, 698
- Graham, J.R. & Dey, A., 1996, ApJ, 471, 720
- Hartwick F.D.A., Schade D., 1990, ARA&A 28, 437
- Heckman, T. & Leitherer, C., 1997, AJ, 114, 69
- Hughes, D.H. et al., 1998, Nature, 394, 241
- Hu, E.M., Cowie, L.L., and McMahon, R.G., 1998, ApJ, 502, L99

- Hu, E.M. & McMahon, R.G., 1996, *Nature*, 382, 231
- Hu, E.M. et al., 1991, *ApJ*, 368, 28
- Kulkarni, S.R. et al., 1998, *Nature*, 393, 35
- Kunth, D., et al., 1998, astro-ph/9809096
- Leitherer, C., Robert, C., & Heckman, T.M., 1995a, *ApJS*, 99, 173
- Leitherer, C., et al., 1995b, *ApJ*, 454, 19L
- Lilly, S.J. et al., 1995a, *ApJ*, 455, 50
- Lilly, S.J. et al., 1995b, *ApJ*, 455, 108
- Liu, C.T. & Kennicutt, R.C., 1995, *ApJ*, 450, 547
- Lowenthal, J.D. et al., 1997, *ApJ*, 481, 673
- Lowenthal, J.D. et al., 1991, *ApJ*, 377, L73
- Macchetto, F.D., et al., 1993, *ApJ*, 404, 511
- Madau, P., 1997, in *The Hubble Deep Field*, eds. M. Livio, S.M. Fall, & P. Madau (Cambridge: Cambridge University Press)
- Madau, P., et al., 1996, *MNRAS*, 283, 1388
- Madau, P., 1995, *ApJ*, 441, 18
- Mannucci, F et al., 1998, *ApJ*, 501, L11
- Meisenheimer, K. et al., 1998, “The Calar Alto Deep Imaging Survey for Galaxies and Quasars at  $z > 5$ ”, in “The young universe: Galaxy formation and evolution at intermediate and high redshift”, S. D’Oderico, A. Fontana, E. Giallongo (eds.), 1998, p. 134-141.
- Meisenheimer, K., et al., 1995, *Galaxies in the Young Universe*, Springer, Berlin Heidelberg New York, 1995, p.273
- Moller, M. & Warren, S.J., 1996, *A&A*, 311, 25
- Neufeld, D., 1991, *ApJ*, 432, 567
- Oke, J.B., et al., 1995, *PASP*, 107, 375
- Osterbrock, 1962, *ApJ*, 135, 195
- Pascarelle, S.M. et al., 1996, *Nature*, 383, 45
- Petitjean, P., et al. 1996, *Nature*, 380, 411
- Pettini, M., et al., 1998, astro-ph/9806219

- Pettini, M., et al., 1997, astro-ph/9708117
- Pritchett, C., 1994, PASP, 106, 1052
- Rawlings, S. et al., 1996, Nature, 383, 502
- Schneider, D.P. et al., 1991, AJ, 102, 837
- Spinrad, H. et al., 1998, astro-ph/9802150
- Steidel, C.C. et al., 1998a, ApJ, 492, 428
- Steidel, C.C. et al., 1998b, astro-ph/9805267
- Steidel, C.C. et al., 1996a, ApJ, 462, L17
- Steidel, C.C. et al., 1996b, AJ, 112, 352
- Steidel, C.C., & Hamilton, D. 1992, AJ, 104, 941
- Steidel, C.C., & Hamilton, D. 1993, AJ, 105, 2017
- Thommes, E. et al., 1998a, MNRAS, 293, L6
- Thommes, E., et al., 1998b, MNRAS, submitted
- Thommes, E., and Meisenheimer, K., 1998c in preparation
- Thommes, E. et al., 1997  
“Search for Primeval Galaxies with the Calar Alto Deep Imaging Survey” in *Reviews in Modern Astronomy*, R.E. Schielicke (ed.), Band 10 (ISBN 3-9805176-0-8), 1997, p. 297
- Thommes, E. & Meisenheimer, K., 1995, in *Galaxies in the Young Universe*, H.Hippelein, K.Meisenheimer & H.-J.Röser (eds.), Proceedings of a Workshop Held at Ringberg Castle, Tegernsee, FRG, September 22-28, 1994, Springer-Verlag 1995, 242-249
- Thompson, D. et al., 1998, submitted to ApJ
- Thompson, D. et al., 1995, AJ, 110, 963
- Trager, S.C. et al., 1997, ApJ, 485, 92
- Warren S.J. et al. 1994, ApJ 421, 412
- Weymann, R.J. et al., 1998, astro-ph/9807208
- Wolf, C., 1998, submitted to A& A

Fig. 1.— Filter system used by Steidel et al. for observing the Lyman continuum break at  $z \sim 3$  together with the model spectrum of a young star forming galaxy taking into account absorption properties of neutral hydrogen in the galaxy itself and the statistical effects of the intervening neutral hydrogen (reproduced from Steidel et al. 1998b)

Fig. 2.— Colour evolution with redshift of galaxies of different spectroscopic type in the  $U_n, G, R$  filter systems used by Steidel et al. to search for Lyman break galaxies (reproduced from Pettini et al. 1997).

Fig. 3.— These redshift histograms are taken from Steidel et al.(1998b) and represent the status of Steidel’s survey for LBGs in May 1998. In each field prominent redshift “spikes” are clearly visible. The light-grey histogram indicates the empirical redshift selection function.

Fig. 4.— Spectra of LBG (shifted to the restframe wavelength).  $\text{Ly-}\alpha$  appears in emission and absorption. There are hints of a correlation between the strength of the metallic interstellar absorption lines and the strength of  $\text{Ly-}\alpha$  absorption and of an anti-correlation with  $\text{Ly-}\alpha$  emission (from Sprinrad et al. 1998)

Fig. 5.— Keck  $B, R$  and  $I$  images of the field around the radio galaxy 6C0140+326 ( $z=4.41$ ) together with a detailed 2-d spectrum showing the  $\text{Ly-}\alpha$  emission line from the galaxy at  $z=5.34$  (RD1) (from Dey et al. 1998). BD3 is the  $B$ -band dropout Dey et al. originally targeted for.

Fig. 6.— Spectrum of the galaxy RD1 at  $z=5.34$  discovered by Dey et al. (1998). The right panel shows a magnification of the wavelength region around the  $\text{Ly-}\alpha$  line. The solid line corresponds to the  $z=5.24$  galaxy RD1 and the dotted one to the  $z=4.02$   $B$ -dropout BD3. Both lines show the expected asymmetry. (from Dey et al., 1998)

Fig. 7.— Demonstration of the veto-filter strategy. Solid boxes indicate the band width and  $5\sigma$  limit of the deepest broad and medium band filters ( $B, R, I_1, I_2$  refer to the scale on the left). The dotted box represents the  $5\sigma$  limit for line detection in the Fabry-Pérot scan, and dashed boxes refer to  $3\sigma$  limits in the veto-filters 466/9, 611/18 and 627/15 (scale on the right). Note that a typical  $\text{Ly-}\alpha$  galaxy at  $z = 5.7$  will only be detected in the Fabry-Pérot, the  $I$ -bands and perhaps the  $R$ -band, whereas a foreground galaxy at  $z = 0.24$  with very strong emission lines should show up in both 466/9, 627/15 and perhaps 611/18.

Fig. 8.— Photometric spectra from the CADIS data (top panel) together with Keck spectra (lower panel) of the same object obtained with the LRIS spectrograph at Keck II and the 1200g/mm grating. The total exposure time is 8400 s (resolution 4 Å per slitwidth). The error bars in wavelength direction of the photometric CADIS spectra correspond to the transmission wavelengths of the CADIS filters. According to the signal in the filter 611/16 and lack of signals in the filters 465/9 and 628/16, the line in the Fabry-Pérot was identified with the [OIII] emission line of a galaxy at  $z=0.6277$ . This classification is confirmed by the Keck spectrum.

Fig. 9.— This diagram shows the surface density of the candidates of Ly- $\alpha$  emitters at  $z=3.4$  reported by Cowie et al. (1998) (points with error bars) together with the limits drawn from the CADIS data so far (marked by CADIS in the diagram) and the limits of the survey for Ly- $\alpha$  emitters at  $z_0 = 4.8$  of Thompson and Djorgovski (1995) (marked by TD in the diagram). We overplot the expectations from a model calculation, which is consistent with these data points and the limits. (Thommes & Meisenheimer, 1998c). CADIS searches for Ly- $\alpha$  emitters at redshifts 4.7, 5.7 and 6.55 and should therefore be able to set firm limits on such model calculations.

Fig. 10.— Optical filter set of the CADIS multi-color survey. They are supplemented by a NIR filter at  $\lambda = 2100$  nm.

Fig. 11.— Comparison between the CADIS number counts and predictions based on the QSO luminosity functions (Boyle et al. 1991, WHO=Warren et al. 1994), cumulative in redshift for  $R < 22$  mag. There is a significant discrepancy at  $z > 2.2$ , where current literature suggests counts drop off (for details see Wolf *et al.* 1998)

Fig. 12.— The left panel shows the full colour-magnitude diagram of the CADIS 16h field. The stepped lines show the mean and  $\pm 2\sigma$  colors for the objects. Right panel: Detail of the region which shows the extremely red objects (EROs). The filled diamonds are low-mass stars in our galaxy. The colour of the ultra luminous infrared galaxy Arp 220 redshifted to  $z=1.5$  is also shown for comparison (open) circle. The filled circle shows the ERO HR10 (Graham & Dey, 1996), which is one of the two examples of EROs studied in detail in the literature. HR10 appears to be a dusty, star-forming galaxy at  $z=1.44$ .

Fig. 13.— The upper diagram shows the volume-averaged star formation rate as a function of redshift (Madau 1997, Pettini et al. 1997) for  $H_0 = 50 \text{ km s}^{-1}$ . Filled squares: measurements from the HDF; circles: measurements from the Canada-France Redshift Survey (Lilly et al. 1995); open triangle: from local  $H\alpha$  survey; open symbols: same values but corrected for dust; **Redshift axis with a selection of high  $z$  objects:** FBG=faint blue galaxies, see review by Ellis (1997); LBGs = Lyman break galaxies, see section 4; Ly- $\alpha$  emitting galaxies ? => see section 5.2; CADIS => redshift intervals in which the Calar Alto Deep Imaging Survey searches for Ly- $\alpha$  emitting galaxies, see section 5.3; EROs = extremely red objects, see section 5.3.5; QSO peak => see section 5.3.5; most distant radio galaxy, Rawlings et al. 1996; most distant quasar, Schneider et al. 1991; (a) emission line objects associated with damped Ly- $\alpha$  and strong metal absorber redshifts, discovered in a narrow-band infrared survey, see Mannucci et al. 1998; (b), (c), (d), (e) damped Ly- $\alpha$  systems detected in emission, see Macchetto et al. 1993, Djorgovski et al. 1996, Moller & Warren 1996, Lowenthal et al. 1991; (f) Ly- $\alpha$  emitter in the field of a quasar => see Hu & McMahon 1996; (g) Ly- $\alpha$  emitting objects observed behind the rich cluster CL0939+4713 (Abell 851), see Trager et al. 1997; (h) sub-galactic, Ly- $\alpha$  emitting clumps with AGN signatures in the field of a weak radio galaxy, see Pascarelle et al. 1996

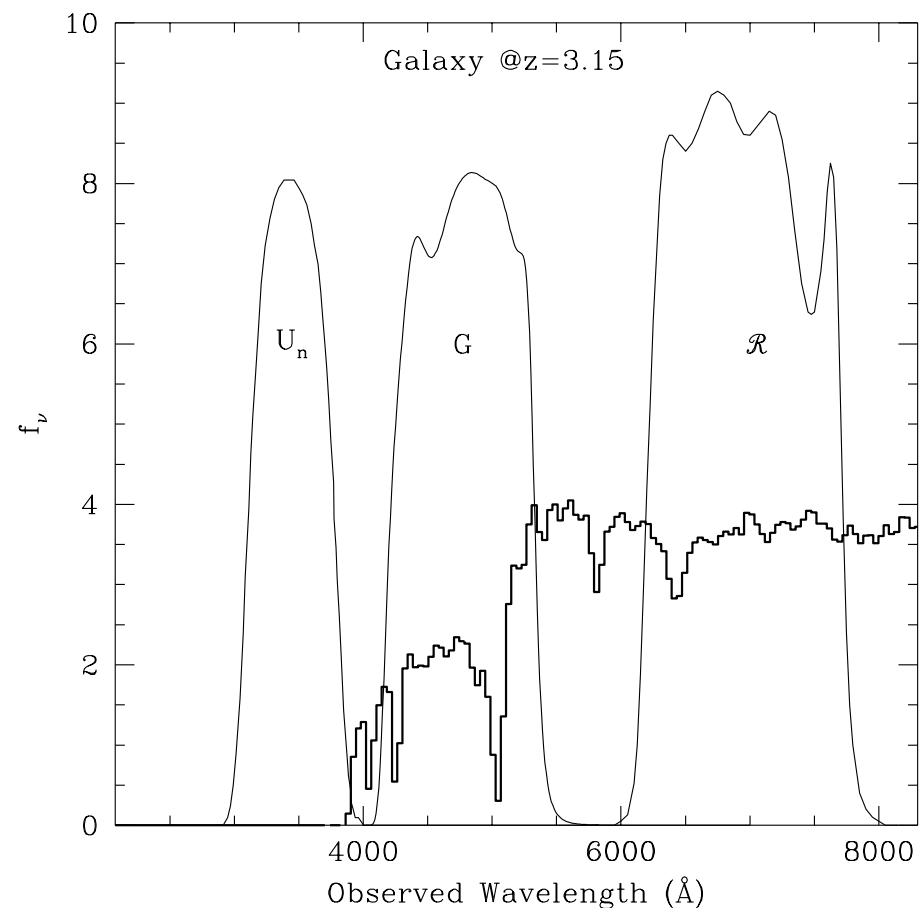


Fig. 1

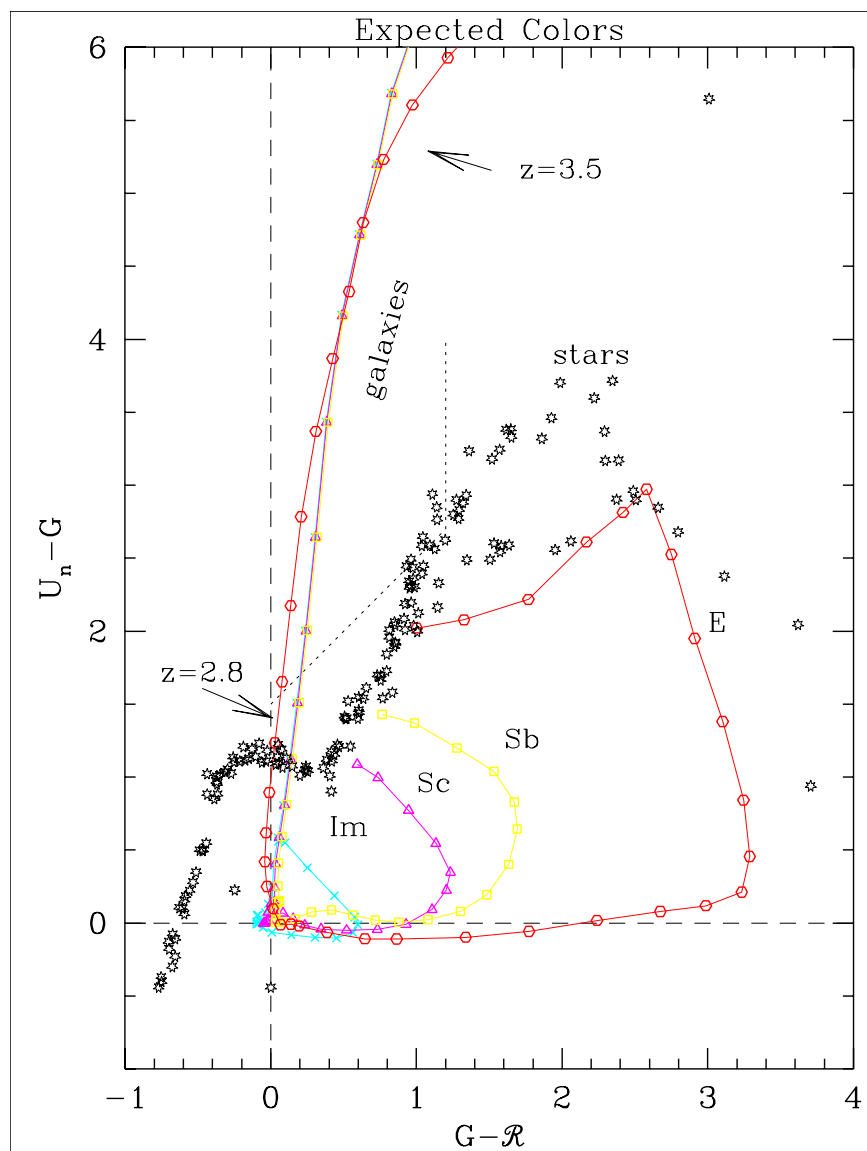


Fig. 2

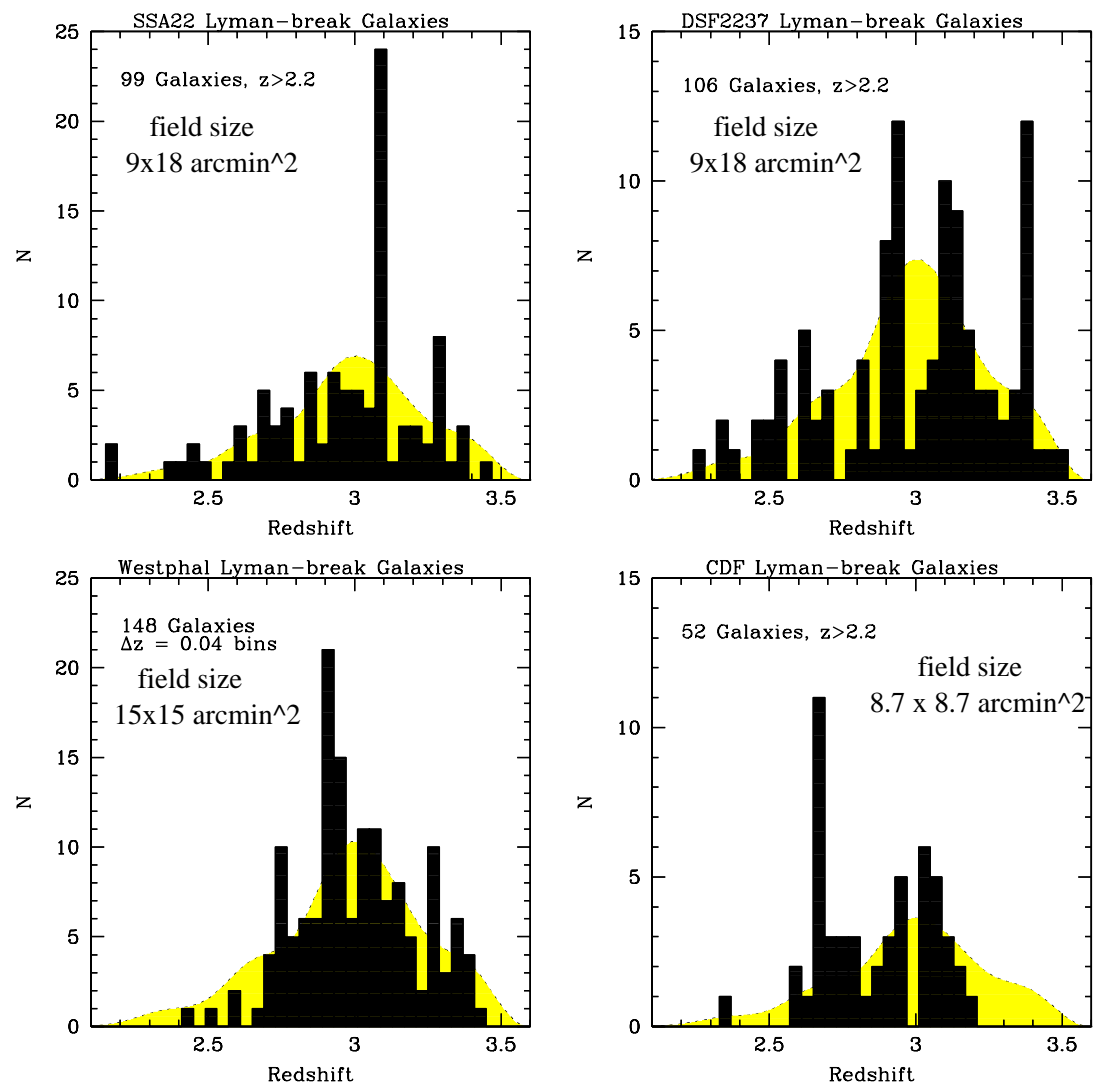


Fig. 3

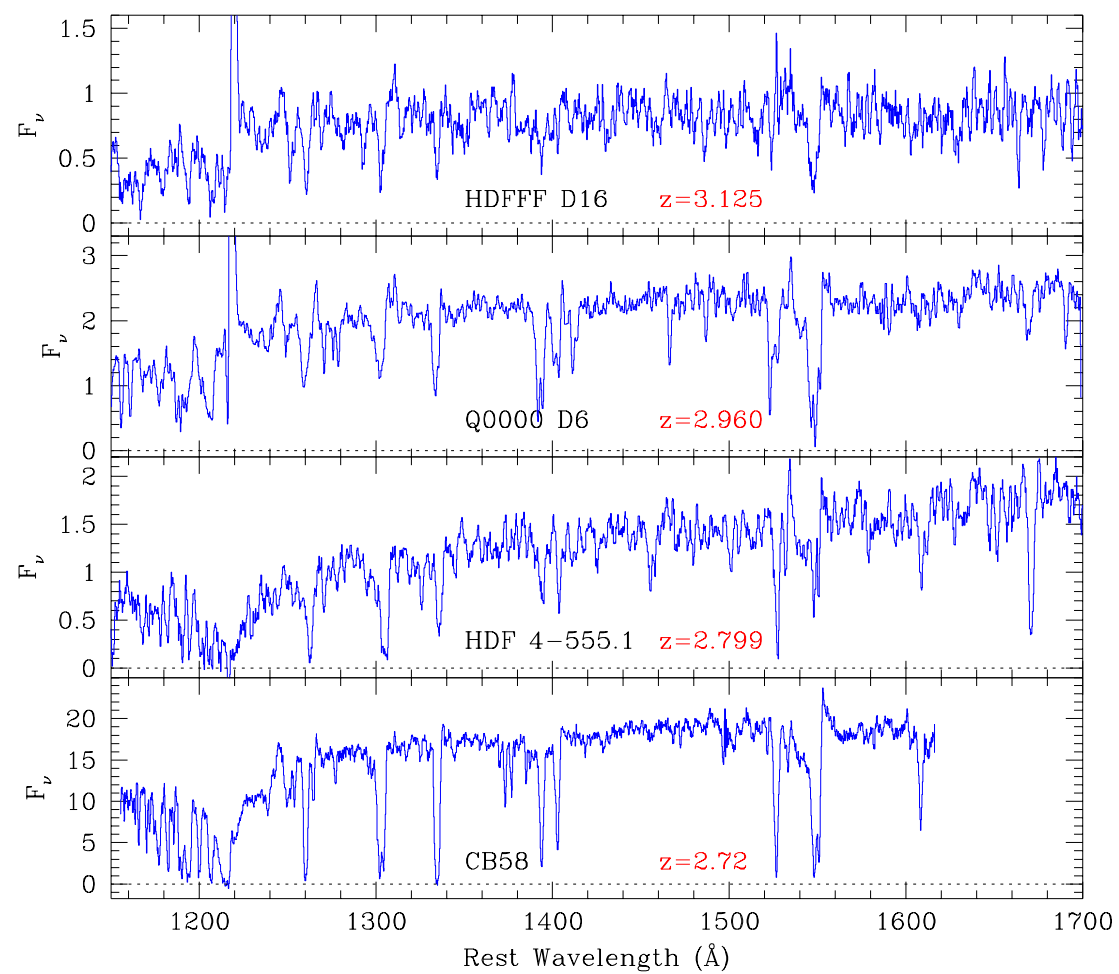


Fig. 4

This figure "figure\_5.gif" is available in "gif" format from:

<http://arxiv.org/ps/astro-ph/9812223v1>

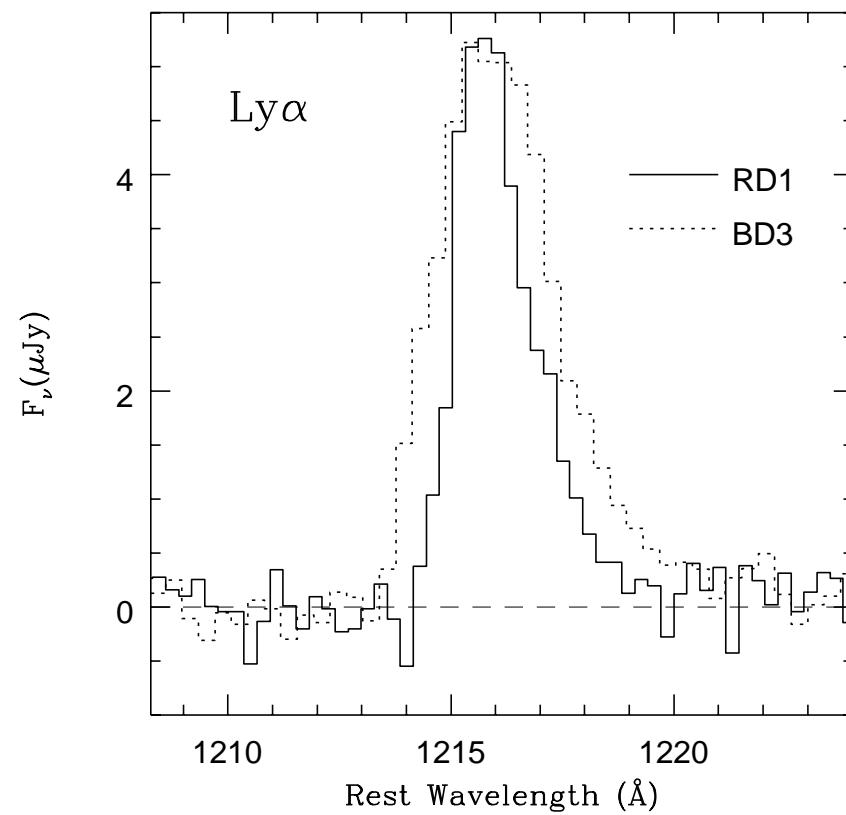
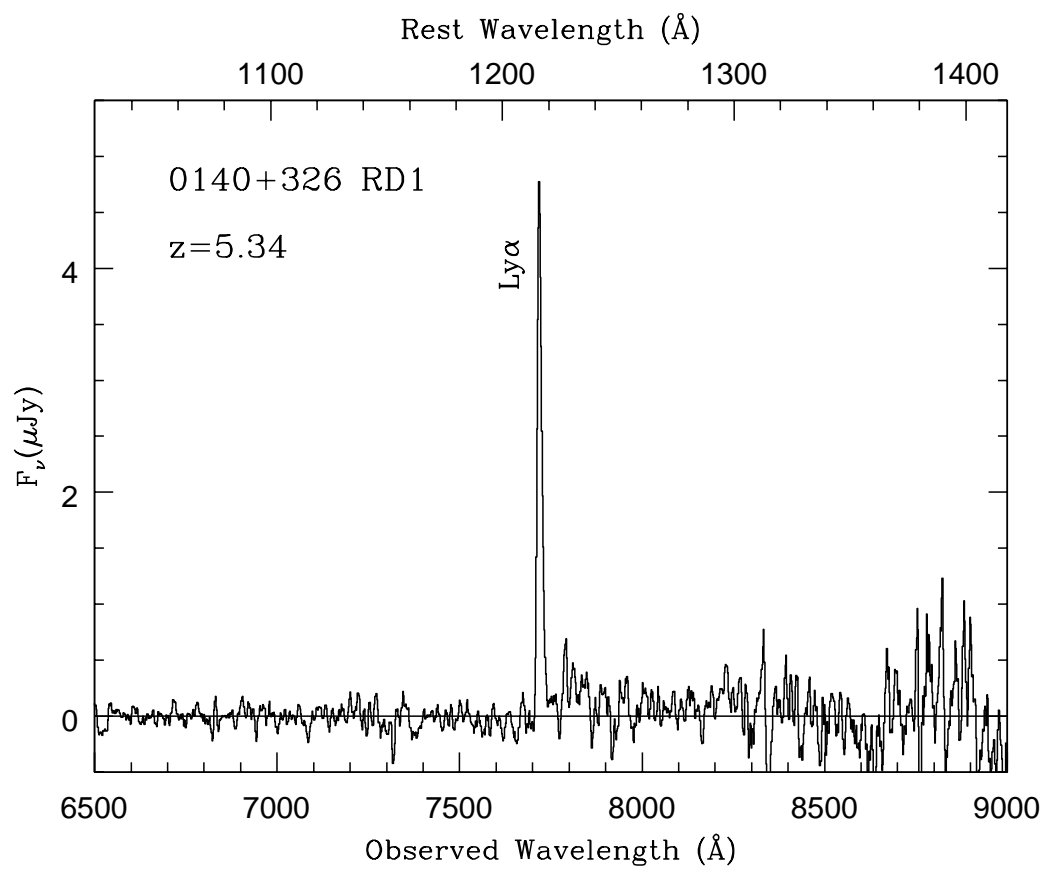
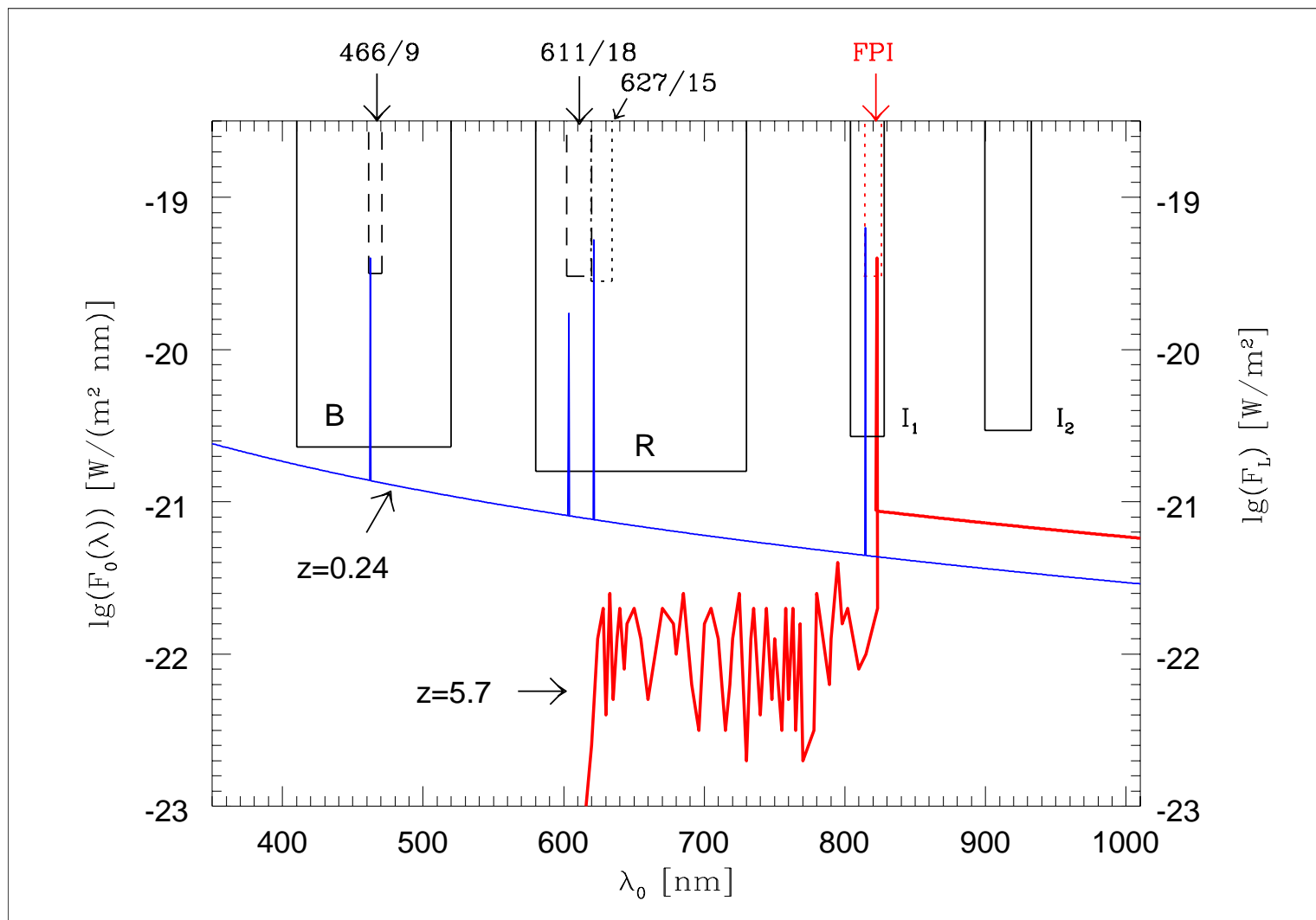


Fig. 6



This figure "figure\_8.gif" is available in "gif" format from:

<http://arxiv.org/ps/astro-ph/9812223v1>

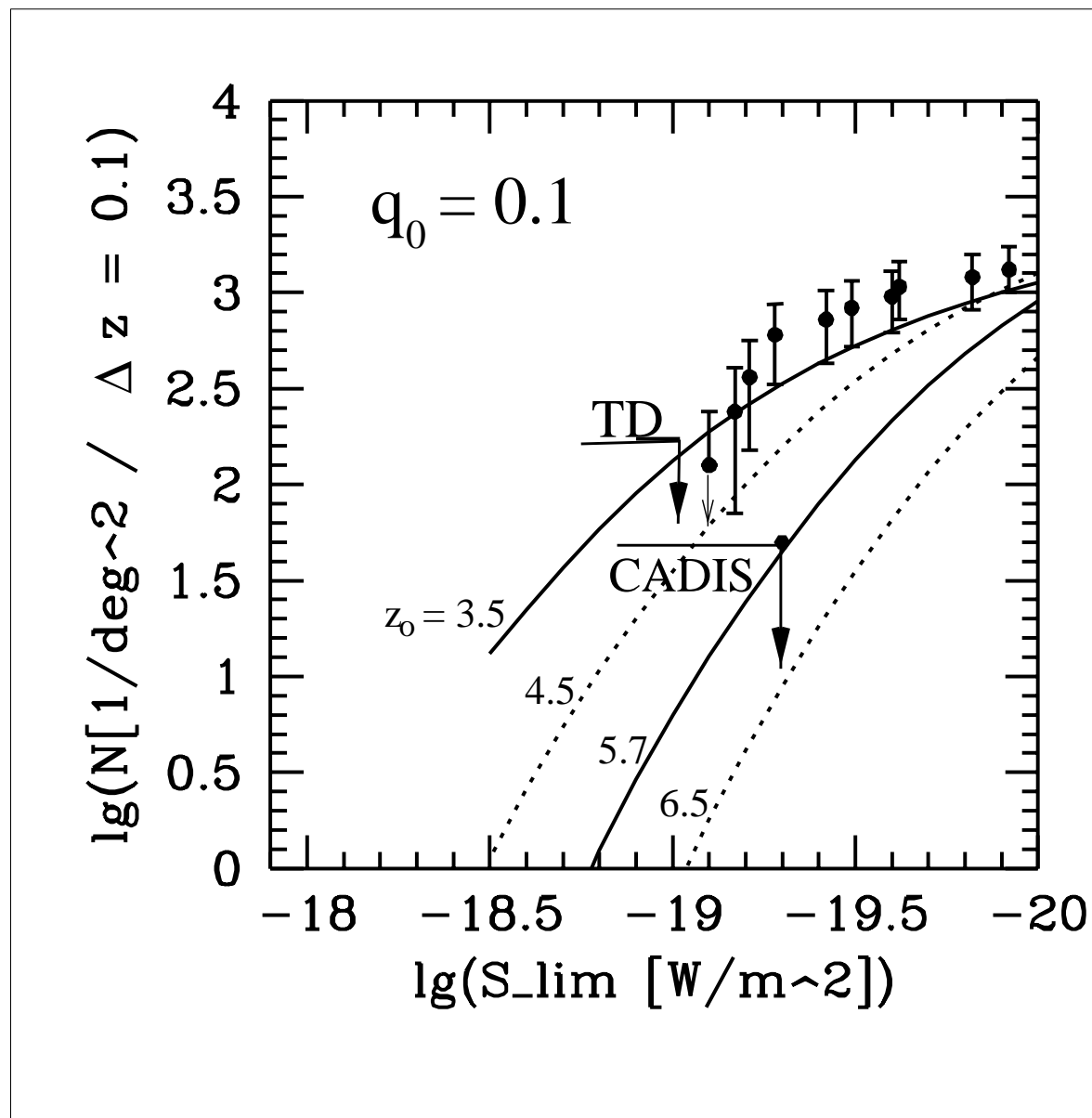


Fig. 9

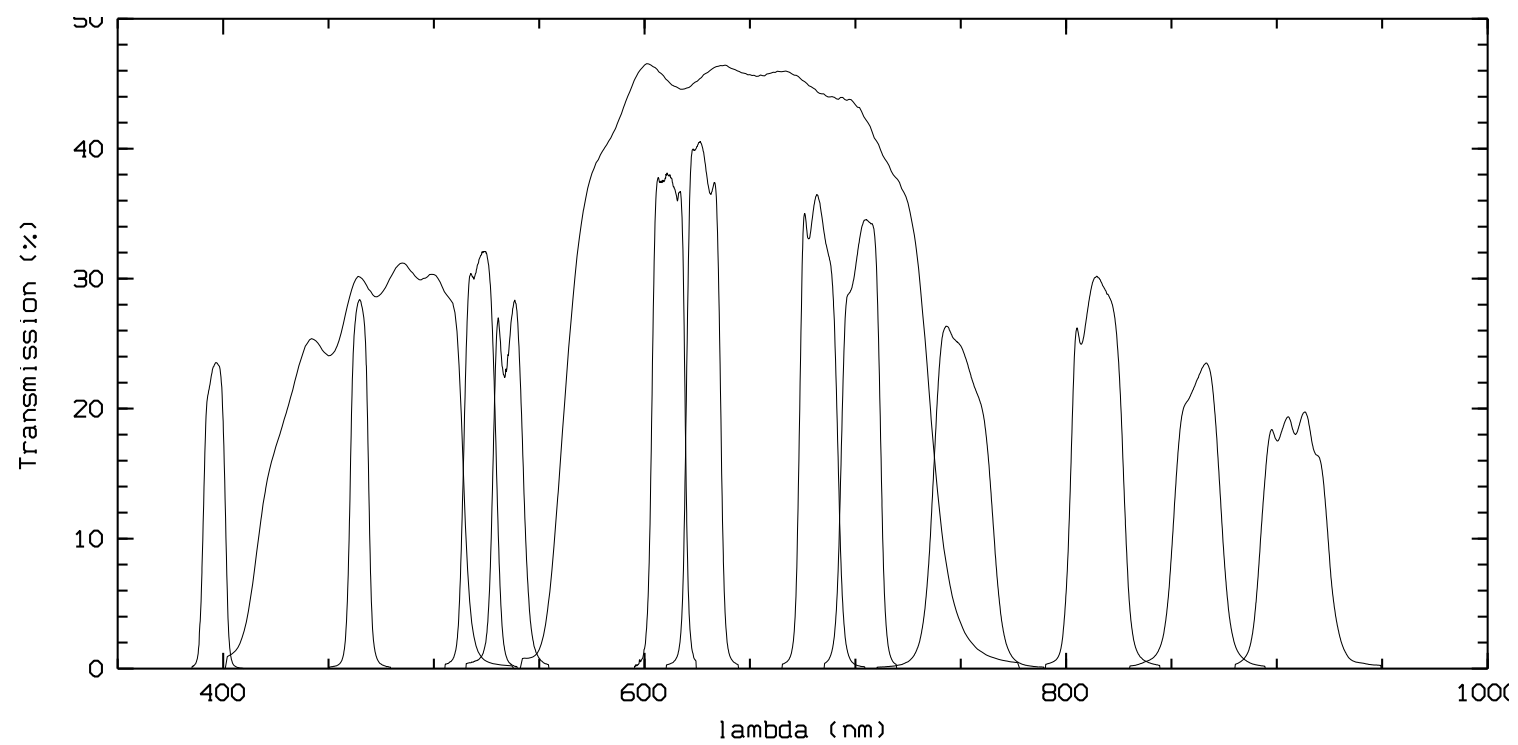


Fig. 10

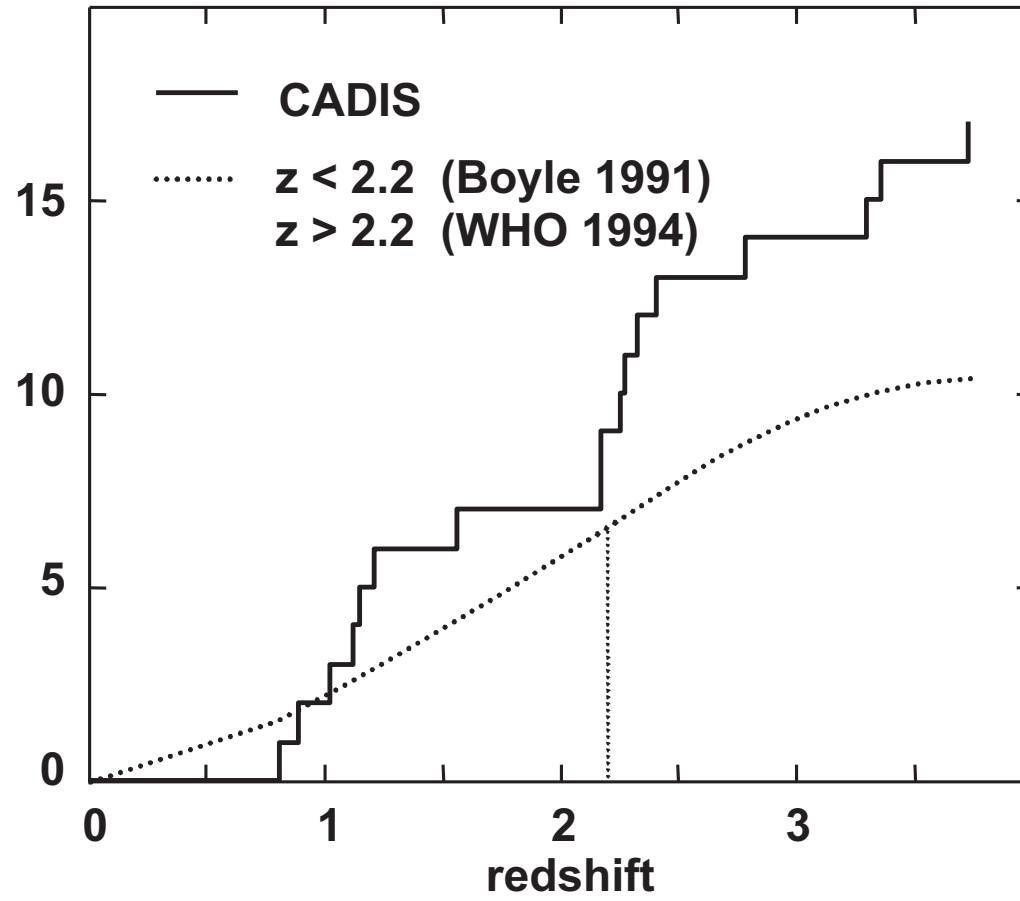


Fig. 11

This figure "figure\_12.gif" is available in "gif" format from:

<http://arxiv.org/ps/astro-ph/9812223v1>

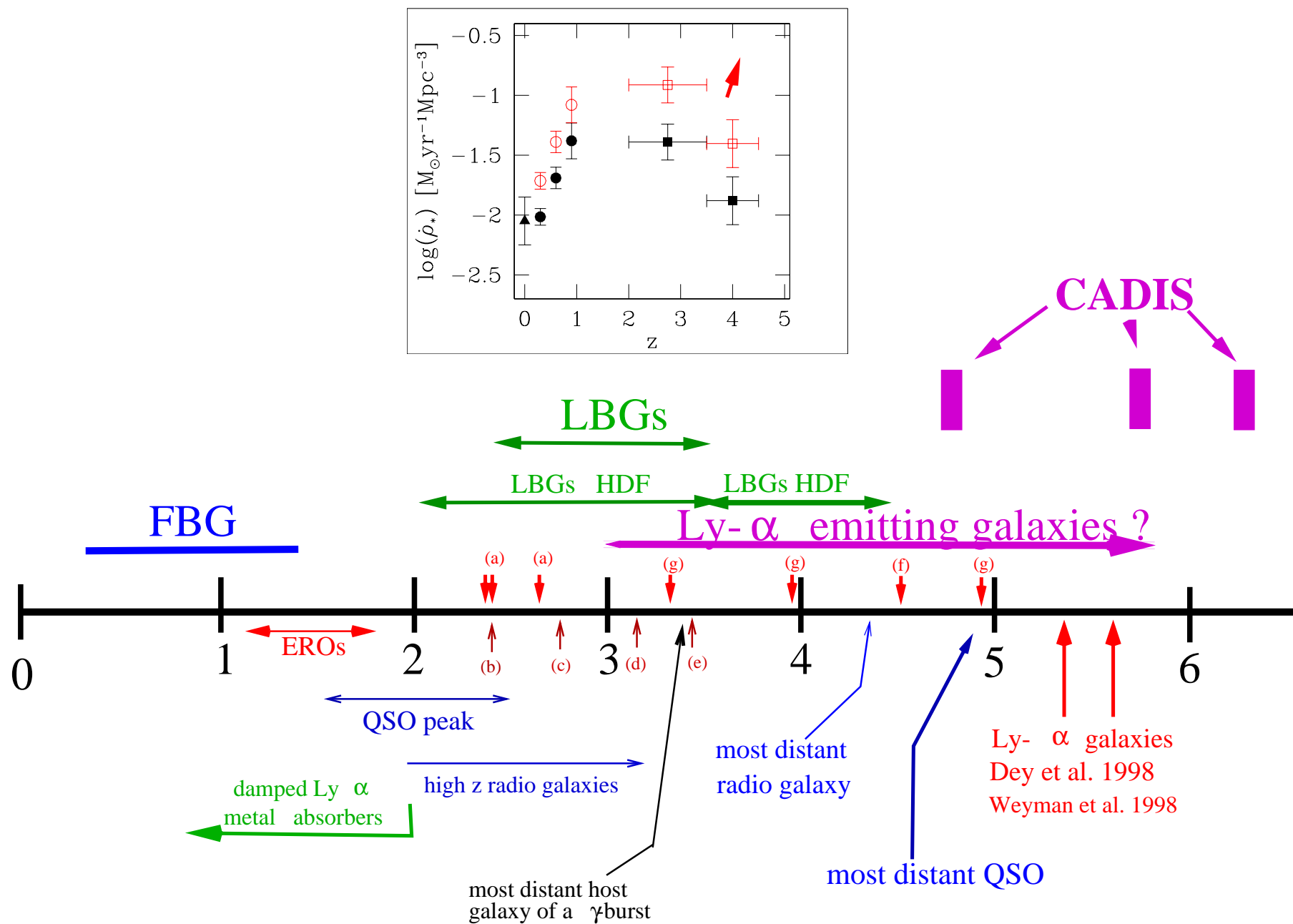


Fig. 13